



VIBRATION ANALYSIS OF ROTATING RINGS WITH INTERNAL PRESSURE AND ELASTIC FOUNDATION USING A SPECTRAL ELEMENT FORMULATION

Danilo Beli

José Roberto de França Arruda

University of Campinas, Faculty of Mechanical Engineering, Department of Computational Mechanics. Rua Mendeleev, 200. CEP:13083-860. Cidade Universitária Zeferino Vaz, Barão Geraldo, Campinas/SP, Brazil.

e-mails: dbeli@fem.unicamp.br, arruda@fem.unicamp.br

Abstract. *This work derives a spectral element for a rotating ring segment with internal pressure, elastic foundation and structural damping that is based on the Euler-Bernoulli beam theory. The rotating effect appears as Coriolis accelerations, which cause the bifurcation of the natural frequencies, and as a centrifugal hoop stress, which causes an increase of the ring stiffness. The internal pressure shift the resonance peaks to higher frequencies making the system more rigid. The elastic foundation causes the bifurcation of the rigid body mode and makes the system stiffer. The structural damping decreases the amplitude of the resonance peaks without modifying the resonance frequencies. The spectrum relation (wavenumber versus frequency) and the forced response are obtained. Results are validated by comparison with the analytical solution for a uniform ring. A rotating dynamic force is naturally derived for the Spectral Element Method and employed to compute the forced response. The models developed in this work can be used to investigate the dynamic behavior of uniform and non-uniform rings*

Keywords: *rotating ring, internal pressure, elastic foundation, wave propagation, spectral element.*

1. INTRODUCTION

Several methods have been used to evaluate the dynamic behavior of structures and the Spectral Element Method (SEM) (Doyle, 1997) is one of them. SEM is a method based on wave propagation with the dynamic stiffness matrix written in the frequency domain. It has similarities with other commonly used methods (Lee, 2009): spatial mesh and assembling of a global matrix using element matrices as in the Finite Element method; exact dynamic description of the structures within the scope of the theory used in the formulation and a reduction of the number of elements that are necessary to describe the structure as in the Dynamic Stiffness Method; superposition of wave propagation modes and the Discrete Fourier Transform used to compute periodic or transient responses via the FFT algorithm as in the Wave Spectral Analysis Method. Therefore, it can be considered as a semi-analytical method.

The main advantage of SEM compared to FEM is that with SEM dynamic models are much smaller and, therefore, can be computed at a much lower computational cost, thus making it more adequate for optimization and uncertainty predictions. Another advantage is eliminating discretization error of the domain that affect the accuracy of the results obtained by FEM in high frequencies. This occurs due to the exact dynamic description in SEM. As a disadvantage, this method is able to calculate only structures with relatively simple geometry.

The flexible rotating ring is an important structural component that has been investigated by several authors (Bickford and Reedy, 1985; Endo, *et al.*, 1984, Huang and Soedel, 1987a and 1987b). They are used to model tires, gears, sensors or when it is necessary to calculate the in-plane vibrations of components that can be approximated by cylinders, such as gas turbines and centrifugal separators, among other applications. The study of tire vibrations due to non-uniformities caused by the fabrication process is the application that has motivated this work.

Endo *et al.* (1984) compared experimental and analytic data for in-plane vibrations of uniform rings. In their formulation, the initial tension due to the rotation and the centrifugal acceleration were considered. Their results were similar to ours for the natural frequencies as a function of rotation speed and showed that, for thin rings, the rotary inertia can be neglected. Bickford and Reedy (1985) derived the equations of motion of a rotating ring using the Euler-Bernoulli theory considering the Coriolis acceleration and the hoop stress induced by the rotation. They concluded that the transverse shear deflection and the rotary inertia can be neglected for thin rings. Huang and Soedel (1987a and 1987b) applied these equations to obtain the free and forced response for stationary rings with rotating loads and for rotating rings with stationary loads to know if the problems were similar. Their analyses concluded that they are similar for low rotating speeds or when the excitation frequency is high compared to the rotation speed.

In a preview work (Beli and Arruda, 2013), the effects of rotation were investigated using a spectral element formulation for a rotating ring. The model is able to simulate the bifurcation of natural frequencies that occurs due the Coriolis acceleration and a shift of the frequencies to higher values of the spectrum that occurs due the centrifugal hoop stress that increase the stiffness with the rotation. Now, the authors consider other effects in the formulation, namely the internal pressure, an elastic foundation and structural damping, which enrich the modeling of the dynamic behavior of rings.

The model is developed only for in-plane vibrations using the Euler-Bernoulli beam theory including the effects of rotation of the previous work (centrifugal acceleration and centrifugal hoop stress), internal pressure, elastic foundation and structural damping. The spectrum relation and the forced response are analyzed and the results are validated for a homogenous ring using an analytical solution. A rotating dynamic force is naturally derived in the formulation and used to compute the forced response.

2. EQUATIONS OF MOTION

A scheme of the rotating curved beam segment with internal pressure and elastic foundation treated here can be seen on Fig. 1.

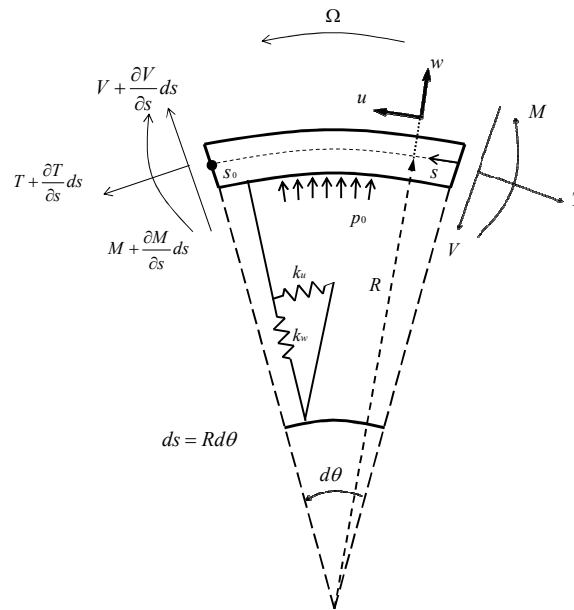


Figure 1. Differential element of rotating ring on an elastic foundation with internal pressure

The Euler-Bernoulli assumption that plane sections remain plane after deformation and normal to the reference surface can be used for thin rings. Neglecting the transverse shear deformation effect, considering that significant strain is therefore in the s direction, and using Hamilton's principle, the coupled equations of motion governing the element may be shown to be (Huang and Soedel 1987b):

$$\begin{aligned}
 & E^* I \left(\frac{\partial^3 u}{\partial s^3} - R \frac{\partial^4 w}{\partial s^4} \right) - E^* A \left(\frac{w}{R} + \frac{\partial u}{\partial s} \right) + (\rho A R \Omega^2 + b p_0) \left(-2R \frac{\partial u}{\partial s} + R^2 \frac{\partial^2 w}{\partial s^2} \right) - (b p_0 + b R k_w) w \\
 & = \rho A R \left(\frac{\partial^2 w}{\partial t^2} - 2\Omega \frac{\partial u}{\partial t} \right) \\
 & E^* I \left(\frac{1}{R} \frac{\partial^2 u}{\partial s^2} - \frac{\partial^3 w}{\partial s^3} \right) + E^* A \left(\frac{\partial w}{\partial s} + R \frac{\partial^2 u}{\partial s^2} \right) + (\rho A R \Omega^2 + b p_0) \left(2R \frac{\partial w}{\partial s} + R^2 \frac{\partial^2 u}{\partial s^2} \right) - (b p_0 + b R k_u) u \\
 & = \rho A R \left(\frac{\partial^2 u}{\partial t^2} + 2\Omega \frac{\partial w}{\partial t} \right)
 \end{aligned} \tag{1}$$

Where

$$E^* = E(1 + i\eta) \tag{2}$$

E is the Young's modulus, η is the structural damping coefficient, w and u are the radial and the tangential displacements, s is the angular coordinate, s_0 is the angular length of the element, t is the time variable, R is the mean radius, b and h are the width and the height of the beam, A is the cross section area, I is the area moment of inertia, ρ is

the mass density, p_0 is the internal pressure, k_w and k_u are the radial and tangential elastic foundation stiffness, and Ω is the rotation velocity. In Fig. (1), T is the axial force, V is the transverse force and M is the bending moment.

In the system of equations Eq. (1), the first equation corresponds to the flexural equation and the second to the extension equation. In these equations the Coriolis terms are $2\Omega(dw/dt)$ and $2\Omega(dw/dt)$ and the tangential and radial velocities are modified by the angular speed, thus modifying the stationary ring problem. The centrifugal hoop stress term is $\rho\Omega^2R^2$; it works as an internal pressure that increases with the rotational velocity.

The internal pressure is modeled in agreement with the thin-walled pressure vessel theory. An elastic foundation links the element with the rotating axes, acting as external forces in the formulation. Equation (2) expresses the structural damping model with the simple introduction of a complex Young's modulus.

3. SPECTRAL ELEMENT FORMULATION

The methodology to model a spectral element for this structural component consists in relating the forces with the displacements in the frequency domain. When one does this, one obtains the dynamic stiffness spectral matrix.

Assuming a wave propagation solution for Eq. (1) as:

$$\begin{aligned} w(s, t) &= C_w e^{i(-\gamma s - \omega t)} \\ u(s, t) &= C_u e^{i(-\gamma s - \omega t)} \end{aligned} \quad (3)$$

Where C_w and C_u are the radial and transverse constants of the solutions, γ is the wave number and ω is the wave propagation frequency.

Calculating the derivatives of the solutions, Eq. (3), and replacing them in Eq. (1), and rearranging the terms, one obtains a system of equations as functions of the amplitudes C_w and C_u :

$$\begin{bmatrix} \left(E^* IR\gamma^4 + \frac{E^* A}{R} + \rho AR^3 \Omega^2 \gamma^2 \right) & -i \left\{ \begin{array}{l} E^* I\gamma^3 + E^* A\gamma - 2\rho AR\omega \\ + 2(\rho AR\Omega^2 + bp_0)R\gamma \end{array} \right\} \\ -i \left\{ \begin{array}{l} E^* I\gamma^3 + E^* A\gamma - 2\rho AR\omega \\ + 2(\rho AR\Omega^2 + bp_0)R\gamma \end{array} \right\} & \left(\frac{-E^* I}{R} \gamma^2 - E^* AR\gamma^2 - \rho AR^2 \Omega^2 \gamma^2 \right) \\ & - (bp_0 + bRk_u) + \rho AR\omega^2 \end{bmatrix} \begin{Bmatrix} C_w \\ C_u \end{Bmatrix} = \begin{Bmatrix} 0 \\ 0 \end{Bmatrix} \quad (4)$$

The determinant of the matrix on the left side of Eq. (4) is calculated and equating it to zero, for the non-trivial solution, one has the characteristic equation, Eq. (5), which relates the wave numbers with frequency.

$$\begin{aligned} & (-E^* AE^* IR^2 - E^* IR^3 bp_0 - \rho AE^* IR^4 \Omega^2) \gamma^6 + (2E^* AE^* I + 2E^* IRbp_0 - E^* IR^2 bk_u - E^* AR^3 bp_0 - R^4 b^2 p_0^2 + \\ & \rho AE^* IR^2 \omega^2 + 3\rho AE^* IR^2 \Omega^2 - \rho AE^* AR^4 \Omega^2 - 2\rho AR^5 bp_0 \Omega^2 - \rho^2 A^2 R^6 \Omega^4) \gamma^4 + (-4\rho AE^* I\Omega\omega) \gamma^3 + \\ & \left(-\frac{E^* AE^* I}{R^2} - \frac{E^* Ibp_0}{R} - E^* Ibk_w + 2E^* ARbp_0 - E^* AR^2 bk_w + 2R^2 b^2 p_0^2 - R^3 b^2 p_0 k_u - R^3 b^2 p_0 k_w + \rho AE^* I\omega^2 + \right. \\ & \left. \rho AE^* AR^2 \omega^2 + 3\rho AE^* AR^2 \Omega^2 + 2\rho AR^3 bp_0 \omega^2 + 6\rho AR^3 bp_0 \Omega^2 - \rho AR^4 bk_u \Omega^2 - \rho AR^4 bk_w \Omega^2 + 2\rho^2 A^2 R^4 \Omega^2 \omega^2 + \right. \\ & \left. 4\rho^2 A^2 R^4 \Omega^4 \right) \gamma^2 + (-4\rho AE^* AR\Omega\omega - 8\rho AR^2 bp_0 \Omega\omega - 8\rho^2 A^2 R^3 \Omega^3 \omega) \gamma + (-b^2 p_0^2 - b^2 R p_0 k_u - b^2 R p_0 k_w - \\ & b^2 R^2 k_u k_w - \frac{E^* A}{R} bp_0 - E^* Abk_u + \rho AE^* A\omega^2 + 2\rho ARbp_0 \omega^2 + \rho AR^2 bk_u \omega^2 - \rho^2 A^2 R^2 \omega^4 + 4\rho^2 A^2 R^2 \Omega^2 \omega^2) = 0 \end{aligned} \quad (5)$$

Rewriting Eq. (5) by grouping terms of similar powers yields:

$$p_6 \gamma^6 + p_4 \gamma^4 + p_3 \gamma^3 + p_2 \gamma^2 + p_1 \gamma + p_0 = 0 \quad (6)$$

Equation (6) shows there are six wave numbers that may be real, imaginary, or complex at each frequency. Three wave numbers represent waves that propagate in the positive/clockwise direction and three waves that propagate in the negative/counterclockwise direction. Because of the Coriolis terms inserted by rotation, the wave numbers that propagate in different directions aren't symmetric, as occurs in the stationary ring treated by Lee et al. (2007). It is necessary to know the propagation direction of the waves to use the previous formulation, which depends on the boundary conditions.

According to Lee et al. (2007), the wave numbers that propagate in the positive direction follow Eq. (7). The positive direction is the same as the direction of rotation of the ring shown in Fig. (1), in other words, the counterclockwise direction.

$$\text{Im}\{\gamma\} \geq 0 \text{ or } \text{Re}\left\{\frac{\partial\gamma}{\partial\omega}\right\} > 0 \text{ if } \text{Im}\{\gamma\} = 0 \quad (7)$$

Using Eq. (5), the derivative of γ with respect to ω may be written as:

$$\frac{\partial\gamma}{\partial\omega} = -\frac{\left[\begin{aligned} &(2\rho AE^* IR^2\omega)\gamma^4 + (-4\rho AE^* IR\Omega)\gamma^3 + (2\rho AE^* I\omega + 2\rho AE^* AR^2\omega + 4\rho AR^3 bp_0\omega + 4\rho^2 A^2 R^4 \Omega^2\omega)\gamma^2 \\ &+ (-4\rho AE^* AR\Omega - 8\rho AR^2 bp_0\Omega - 8\rho^2 A^2 R^3 \Omega^3)\gamma + (2\rho AE^* A\omega - 4\rho^2 A^2 R^2\omega^2 + 8\rho^2 A^2 R^2 \Omega^2\omega) \end{aligned} \right]}{6p_6\gamma^5 + 4p_4\gamma^3 + 3p_3\gamma^2 + 2p_2\gamma + p_1} \quad (8)$$

Equation (6) yields six wave numbers, and using Eq. (7) one can separate them, defining that the wave numbers γ_1 , γ_2 and γ_3 propagate in the positive direction and γ_4 , γ_5 and γ_6 propagate in the negative direction.

Thus, the displacements can be written for each frequency as:

$$w(s,t) = (C_{w1}^+ e^{-i\gamma_1 s} + C_{w2}^+ e^{-i\gamma_2 s} + C_{w3}^+ e^{-i\gamma_3 s} + C_{w4}^- e^{-i\gamma_4 s} + C_{w5}^- e^{-i\gamma_5 s} + C_{w6}^- e^{-i\gamma_6 s}) e^{-i\omega t} \quad (9)$$

$$u(s,t) = (C_{u1}^+ e^{-i\gamma_1 s} + C_{u2}^+ e^{-i\gamma_2 s} + C_{u3}^+ e^{-i\gamma_3 s} + C_{u4}^- e^{-i\gamma_4 s} + C_{u5}^- e^{-i\gamma_5 s} + C_{u6}^- e^{-i\gamma_6 s}) e^{-i\omega t} \quad (10)$$

The methodology used here to define the spectral matrix is the same employed by Delamotte et al. (2008). In other words, one writes the element displacements as a function of the wave amplitudes in Eq. (9) and writes the element forces and moments as a function of these same wave amplitudes. With these two relations, one can eliminate the wave amplitudes and obtain an expression that relates the displacements and the forces, which yield the desired dynamic stiffness matrix. A way to simplify the equation is to relate the amplitudes of the Eq. (9) and (10). From the system of Eq. (4) one can write:

$$\alpha = \frac{C_u}{C_w} = \frac{E^* IR\gamma^4 + \frac{E^* A}{R} + (\rho AR\Omega^2 + bp_0)R^2\gamma^2 + (bp_0 + bRk_w) - \rho AR\omega^2}{i\{E^* I\gamma^3 + E^* A\gamma + 2(\rho AR\Omega^2 + bp_0)R\gamma - 2\rho AR\Omega\omega\}} \quad (11)$$

or

$$\alpha = \frac{C_u}{C_w} = \frac{i\{E^* I\gamma^3 + E^* A\gamma + 2(\rho AR\Omega^2 + bp_0)R\gamma - 2\rho AR\Omega\omega\}}{-\frac{E^* I}{R\gamma^2} - E^* AR\gamma^2 - (\rho AR\Omega^2 + bp_0)R^2\gamma^2 - (bp_0 + bRk_u) + \rho AR\omega^2}$$

For each wave number there is a different relation, so:

$$\alpha_1 = \frac{C_{u1}^+}{C_{w1}^+}; \alpha_2 = \frac{C_{u2}^+}{C_{w2}^+}; \alpha_3 = \frac{C_{u3}^+}{C_{w3}^+}; \alpha_4 = \frac{C_{u4}^-}{C_{w4}^-}; \alpha_5 = \frac{C_{u5}^-}{C_{w5}^-}; \alpha_6 = \frac{C_{u6}^-}{C_{w6}^-} \quad (12)$$

A matrix $[\alpha]$, a vector $\{C\}$ and a vector $\{N\}$ can be used to write the displacements $w(s)$ and $u(s)$ and the rotation in a simplified form, as functions of the $w(s)$ constants.

$$[\alpha] = \begin{bmatrix} \alpha_1 & 0 & 0 & 0 & 0 & 0 \\ 0 & \alpha_2 & 0 & 0 & 0 & 0 \\ 0 & 0 & \alpha_3 & 0 & 0 & 0 \\ 0 & 0 & 0 & \alpha_4 & 0 & 0 \\ 0 & 0 & 0 & 0 & \alpha_5 & 0 \\ 0 & 0 & 0 & 0 & 0 & \alpha_6 \end{bmatrix} \quad \{C\} = \begin{bmatrix} C_{w1} \\ C_{w2} \\ C_{w3} \\ C_{w4} \\ C_{w5} \\ C_{w6} \end{bmatrix} = \begin{bmatrix} C_1 \\ C_2 \\ C_3 \\ C_4 \\ C_5 \\ C_6 \end{bmatrix} \quad \{N\} = \begin{bmatrix} e^{-i\gamma_1 s} \\ e^{-i\gamma_2 s} \\ e^{-i\gamma_3 s} \\ e^{-i\gamma_4(s-s_0)} \\ e^{-i\gamma_5(s-s_0)} \\ e^{-i\gamma_6(s-s_0)} \end{bmatrix} \quad (13)$$

$\{N\}$ is a vector of the spatial solutions for the negative wave numbers, where the s_0 term is the element length, used in order to improve the numeric stability of the solution. Thus, one can write:

$$w(s) = \{N^t(s)\} \{C\} \quad u(s) = \{N(s)\}^t [\alpha] \{C\} \quad w'(s) = \frac{\partial w}{\partial s} = \{N'(s)\}^t \{C\} \quad (14)$$

Evaluating the displacements at the ends of the element, a matrix is found that relates the displacements with the vector of amplitudes $\{C\}$.

$$\begin{Bmatrix} u(0) \\ w(0) \\ w'(0) \\ u(s_0) \\ w(s_0) \\ w'(s_0) \end{Bmatrix} = \begin{bmatrix} \alpha_1 & \alpha_2 & \alpha_3 & \alpha_4 e^{-i\gamma_4 s_0} & \alpha_5 e^{-i\gamma_5 s_0} & \alpha_6 e^{-i\gamma_6 s_0} \\ 1 & 1 & 1 & e^{-i\gamma_4 s_0} & e^{-i\gamma_5 s_0} & e^{-i\gamma_6 s_0} \\ -i\gamma_1 & -i\gamma_2 & -i\gamma_3 & -i\gamma_4 e^{-i\gamma_4 s_0} & -i\gamma_5 e^{-i\gamma_5 s_0} & -i\gamma_6 e^{-i\gamma_6 s_0} \\ \alpha_1 e^{-i\gamma_1 s_0} & \alpha_2 e^{-i\gamma_2 s_0} & \alpha_3 e^{-i\gamma_3 s_0} & \alpha_4 & \alpha_5 & \alpha_6 \\ e^{-i\gamma_1 s_0} & e^{-i\gamma_2 s_0} & e^{-i\gamma_3 s_0} & 1 & 1 & 1 \\ -i\gamma_1 e^{-i\gamma_1 s_0} & -i\gamma_2 e^{-i\gamma_2 s_0} & -i\gamma_3 e^{-i\gamma_3 s_0} & -i\gamma_4 & -i\gamma_5 & -i\gamma_6 \end{bmatrix} \begin{Bmatrix} C_1 \\ C_2 \\ C_3 \\ C_4 \\ C_5 \\ C_6 \end{Bmatrix} \quad (15)$$

Simplifying the notation:

$$\{U(\omega)\} = [G(\omega)] \{C\} \quad (16)$$

It is possible to write the forces as a function of the $\{C\}$ vector too. The forces and moments are related to the deformations and displacements by the Euler-Bernoulli theory. Writing them as functions of the wave amplitudes yields:

$$T = EA \left(\frac{\partial u}{\partial s} + \frac{w}{R} \right) = EA (\{N(s)'\}^t [\alpha] + \{N(s)\}^t) \{C\} \quad (17)$$

$$V = EI \left(\frac{1}{R} \frac{\partial^2 u}{\partial s^2} - \frac{\partial^3 w}{\partial s^3} \right) = EI \left(\frac{1}{R} \{N(s)''\}^t [\alpha] - \{N(s)'''\}^t \right) \{C\} \quad (18)$$

$$M = EI \left(\frac{1}{R} \frac{\partial u}{\partial s} - \frac{\partial^2 w}{\partial s^2} \right) = EI \left(\frac{1}{R} \{N(s)'\}^t [\alpha] - \{N(s)''\}^t \right) \{C\} \quad (19)$$

Evaluating the forces and moments at the ends of the element, a matrix that relates the displacements with the vector of wave amplitudes $\{C\}$ can be obtained:

$$\begin{Bmatrix} -T(0) \\ V(0) \\ -M(0) \\ T(s_0) \\ -V(s_0) \\ M(s_0) \end{Bmatrix} = \begin{bmatrix} -EA[N''^t(0)\alpha + N^t(0)] \\ EI[(1/R)N''''^t(0)\alpha - N''''^t(0)] \\ -EI[(1/R)N''^t(0)\alpha - N''^t(0)] \\ EA[N''^t(s_0)\alpha + N^t(s_0)] \\ EI[(1/R)N''''^t(s_0)\alpha - N''''^t(s_0)] \\ -EI[(1/R)N''^t(s_0)\alpha - N''^t(s_0)] \end{bmatrix} \begin{Bmatrix} C_1 \\ C_2 \\ C_3 \\ C_4 \\ C_5 \\ C_6 \end{Bmatrix} \quad (20)$$

Simplifying the notation:

$$\{F(\omega)\} = [H(\omega)] \{C\} \quad (21)$$

Thus, the spectral matrix for a rotating ring element $[K(\omega)]$ can be obtained from Eq. (16) and Eq. (21):

$$\{F(\omega)\} = [H(\omega)][G(\omega)]^{-1} \{U(\omega)\} = [K(\omega)] \{U(\omega)\} \Rightarrow [K(\omega)] = [H(\omega)][G(\omega)]^{-1} \quad (22)$$

The procedure to assemble the global matrix is the same employed in the Finite Element method, i.e., the superposition of element matrices. The force vector is in the frequency domain and, given the formulation employed, the forces have the same angular speed of the ring and are stationary in a rotating frame, remaining at the nodes when they are applied while they rotate, Fig. 2.

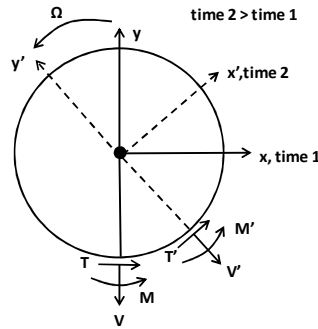


Figure 2. Rotating ring with rotating dynamic loads

With the spectral matrix previously formulated and defining the dynamic force vector, one can obtain the displacements and rotations at each node. The forced response represented by Frequency Response Functions (FRF) can be computed and compared with the results obtained via analytical solution for the homogeneous ring case.

4. ANALYTICAL SOLUTION

Equations (1) are also the equations of motion for a complete ring. The analytical natural frequencies are obtained assuming that the displacements are given by:

$$w(s,t) = W_n e^{i(n\frac{s}{R} + \omega_n t)} \quad (23)$$

$$u(s,t) = U_n e^{i(n\frac{s}{R} + \omega_n t)}$$

Where n is the mode count, W_n and U_n the amplitudes of the solutions. Inserting Eq. (23) in Eq. (1) yields the matrix system:

$$\begin{bmatrix} L_{11} & L_{12} \\ L_{21} & L_{22} \end{bmatrix} \begin{Bmatrix} W_n \\ U_n \end{Bmatrix} = \begin{Bmatrix} 0 \\ 0 \end{Bmatrix} \quad (24)$$

Where

$$L_{11} = \frac{EI}{R^3} n^4 + \frac{EA}{R} + (\rho AR \Omega^2 + bp_0) n^2 + (bp_0 + bRk_w) - \rho AR \omega_n^2$$

$$L_{22} = \frac{EI}{R^3} n^2 + \frac{EA}{R} n^2 + (\rho AR \Omega^2 + bp_0) n^2 + (bp_0 + bRk_u) - \rho AR \omega_n^2 \quad (25)$$

$$L_{12} = -L_{21} = i \left\{ \frac{EI}{R^3} n^3 + \frac{EA}{R} n + 2(\rho AR \Omega^2 + bp_0) n - 2\rho AR \Omega \omega_n \right\}$$

For a non-trivial solution, it is necessary that the determinant of matrix L vanishes, resulting in a polynomial equation (Eq. 26) that yields four natural frequencies: two flexural modes and two extensional modes.

$$l_4 \omega_n^4 + l_2 \omega_n^2 + l_1 \omega_n + l_0 = 0 \quad (26)$$

Finally, the coefficients of Eq. (26) are:

$$l_4 = \rho^2 A^2 R^2 \quad l_2 = -\rho AR(C_1 + C_2) - 4\rho^2 A^2 R^2 \Omega^2 \quad l_1 = 4\rho ARC_3 \quad l_0 = C_1 C_2 - C_3^2 \quad (27)$$

Where

$$C_1 = \frac{EI}{R^3} n^4 + \frac{EA}{R} + (\rho AR \Omega^2 + bp_0) n^2 + (bp_0 + bRk_w)$$

$$C_2 = \frac{EI}{R^3} n^2 + \frac{EA}{R} n^2 + (\rho AR \Omega^2 + bp_0) n^2 + (bp_0 + bRk_u) \quad (28)$$

$$C_3 = \frac{EI}{R^3} n^3 + \frac{EA}{R} n + 2(\rho AR \Omega^2 + bp_0) n$$

5. NUMERICAL RESULTS

The numerical validation of the rotating ring element is done for a uniform rotating ring by comparison of the forced and operational responses with the analytical solution and with a finite element model. The geometric properties of the uniform ring are radius $R = 0.25$ m, width $b = 0.15$ m, height $h = 0.002$ m, mass density $\rho = 7200$ kg/m³, Young's modulus $E = 220$ GPa, rectangular cross-sectional area $A = bh$ and inertia $I = bh^3/12$.

The SE model consists of four spectral elements (Fig. 3a). The forced responses are calculated for a radial excitation force and a radial displacement at the same node as show in Fig. 3b.

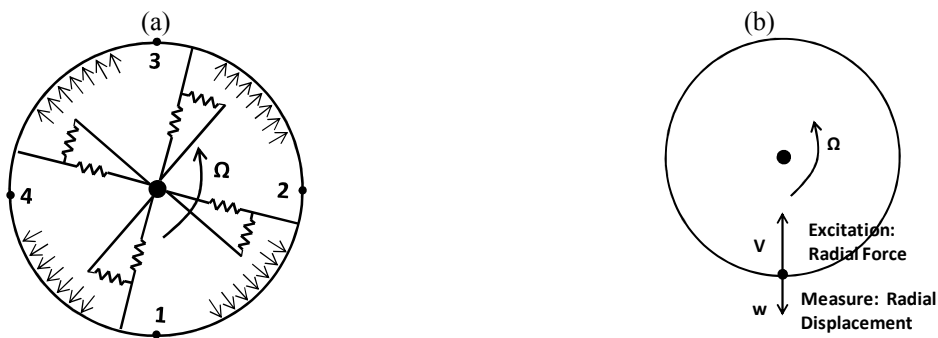


Figure 3. Model of a rotating ring in SEM (a), excitation and response location to calculate the forced response (b).

5.1 Internal Pressure

Using internal pressure of 1 bar with rotation of 50 rad/s the effect of the internal pressure will be investigated. The elastic foundation and structural damping effects are not considered in this sub-section.

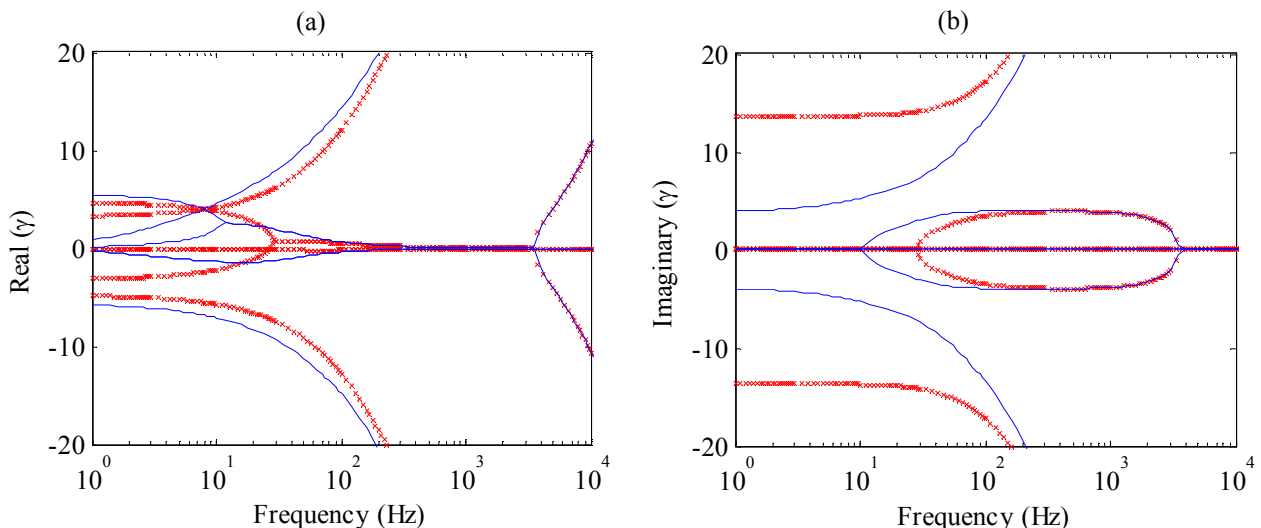


Figure 4. Real (a) and imaginary (b) parts of wavenumbers for $p_0 = 1$ bar (x) and $p_0 = 0$ (-).

The internal pressure influences low and mid frequencies of the spectrum relation (Fig. 4a, Fig. 4b), modifying the real and imaginary parts of the wavenumbers. They are zero until a given frequency, in this case 103 Hz. In the FRF of Fig. 5 the resonance peaks are shifted to higher frequencies in accord with the increasing of the internal pressure. This occurs because the internal pressure increases the ring stiffness.

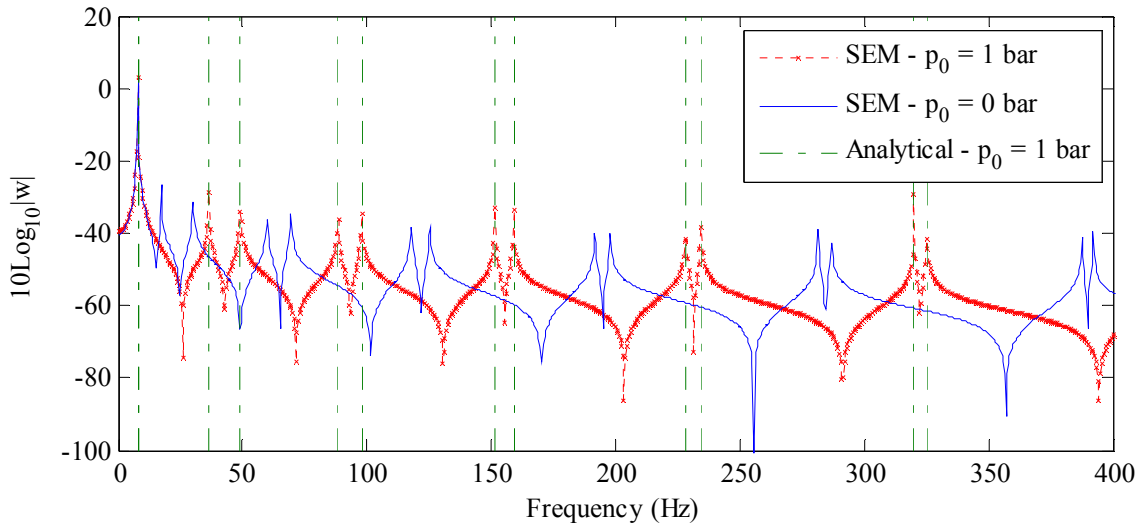


Figure 5. FRFs for internal pressure analysis: SEM for $p_0 = 1$ bar (-x-), SEM for $p_0 = 0$ bar (—) and analytical solution for $p_0 = 1$ bar (vertical lines).

The map of the FRF amplitude versus Ω with internal pressure (Fig. 6a) remains the same as the map of the FRF versus Ω without pressure, but the resonance peaks are shift to higher frequencies because of the internal pressure. In the FRF plot versus internal pressure with constant rotation velocity of 50 rad/s (Fig. 6b) the effect of the internal pressure that is not linear and changes with frequency. The pair of frequencies of bifurcation due the rotation follows the same trend and the high frequency modes are more influenced by the internal pressure. As expected, the rigid body mode does not change with this parameter.

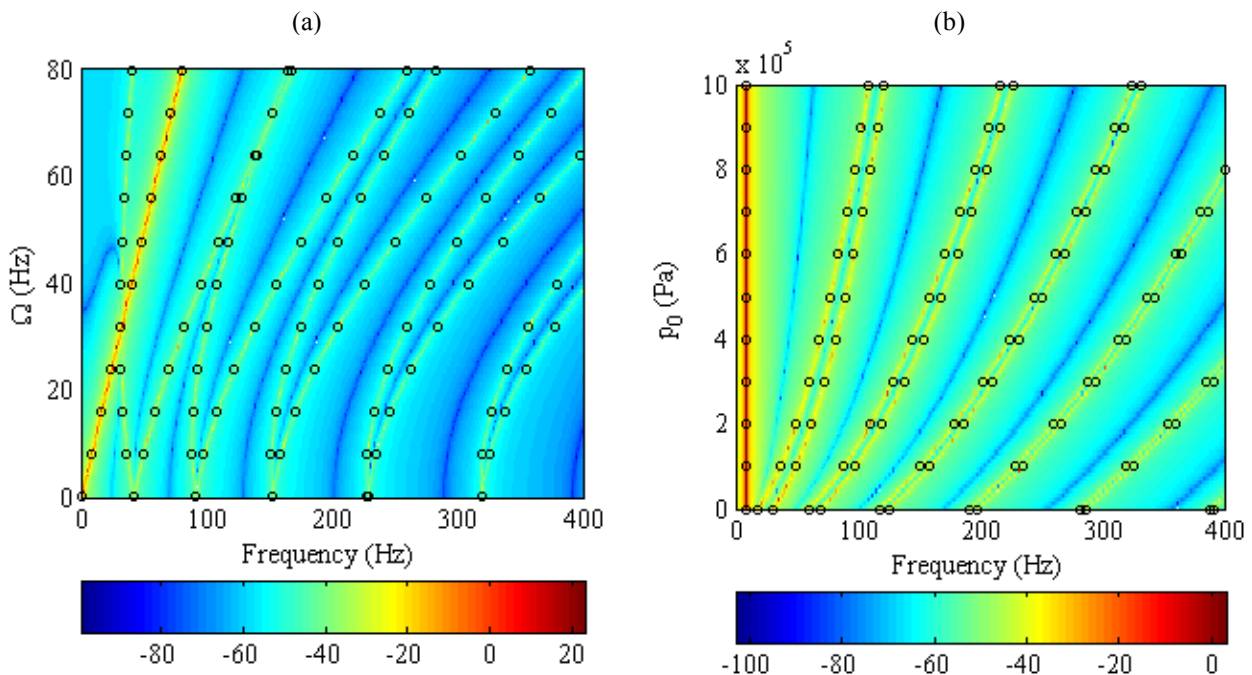


Figure 6. Map of FRF versus Ω with $p_0 = 1$ bar (a) and map of FRF versus internal pressure with $\Omega = 50$ rad/s (b): SEM (continuous map) and analytical solution (o).

5.2 Elastic Foundation

In this sub-section an elastic foundation with radial and tangential values of stiffness spring of 10^4 N/m^3 is included with a rotating speed of 50 rad/s. The internal pressure and structural damping effects are not considered.

The elastic foundation changes the spectrum relation at low frequencies. In this case it slightly modifies the real and imaginary parts of wavenumbers in the range of 0 to 100 Hz (Fig 7a, Fig. 7b). The bifurcation of the rigid body mode caused by the elastic foundation can be seen in the FRF of Fig. 8. Two frequencies corresponding to the radial and tangential stiffness of the foundation appear. The flexural modes in low frequencies are slightly shifted to the right of the spectrum, i.e. the system becomes stiffer.

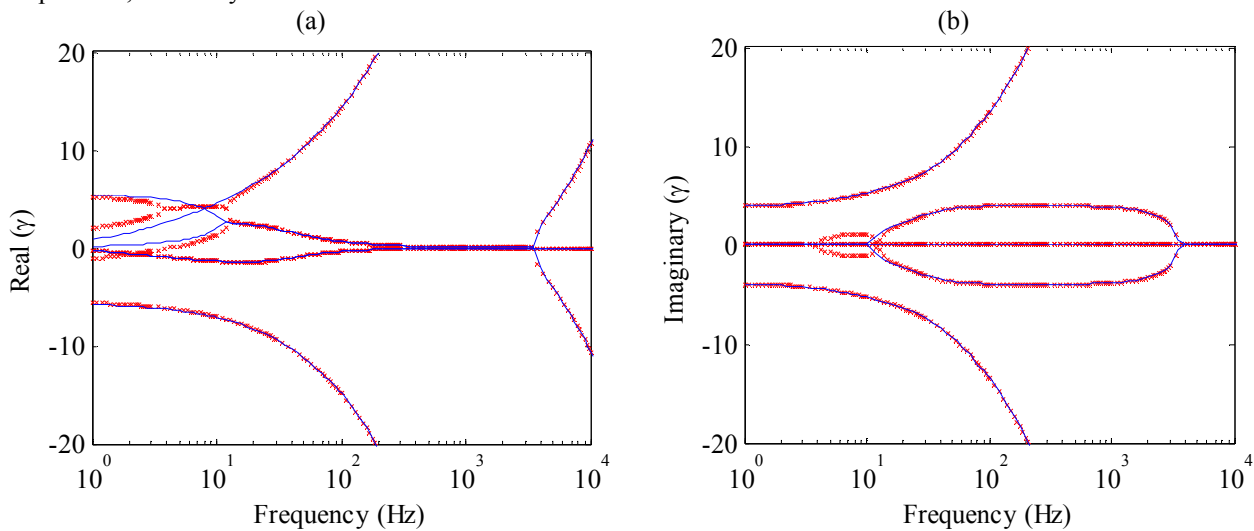


Figure 7. Real (a) and imaginary (b) parts of wavenumbers: $k_w = k_u = 10^4 \text{ N/m}^3$ (x) and $k_w = k_u = 0$ (-).

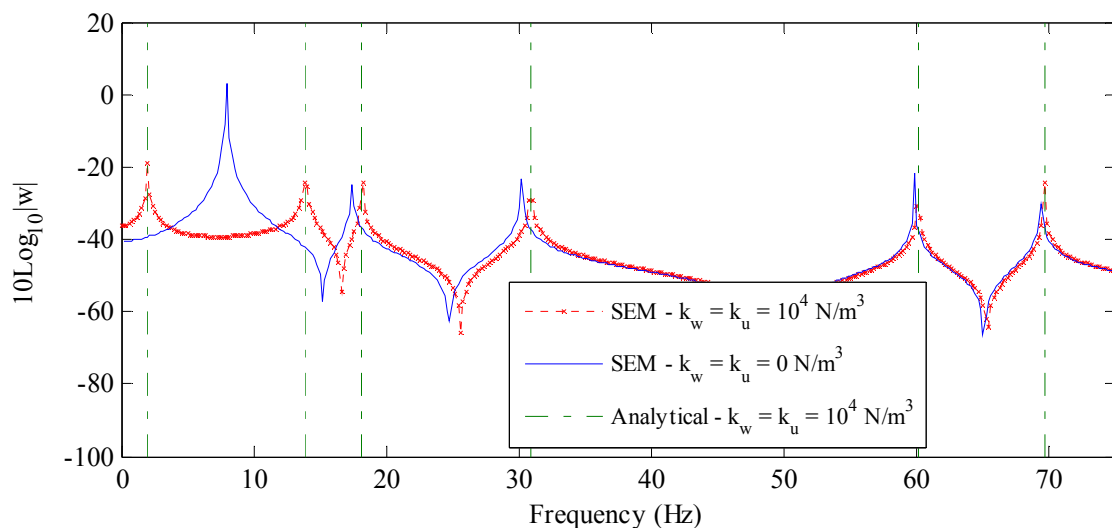


Figure 8. FRF for elastic foundation analysis: SEM for $k_w = k_u = 10^4 \text{ N/m}^3$ (-x-), SEM for $k_w = k_u = 0$ (—) and analytical solution for $k_w = k_u = 10^4 \text{ N/m}^3$ (vertical lines).

In the map of the FRF versus Ω with elastic foundation (Fig. 9a) a bifurcation of the rigid body mode appears, which remains linear with the rotation, but the rotation does not act in the bifurcation of this mode and the bifurcation gap keeps the same ratio with the rotation speed. With foundation stiffness and Ω equal to zero, the system behaves as a mass-stiffness problem with the radial and tangential springs in parallel. Then, the rigid body modes do not start at zero and the two natural frequencies have the same value.

In the analysis of the FRFs versus stiffness of the elastic foundation (Fig. 9b), it is considered that the radial and tangential stiffness have the same value. The bifurcation of the rigid body mode is nonlinear with the spring stiffness, while the other modes have a linear relation.

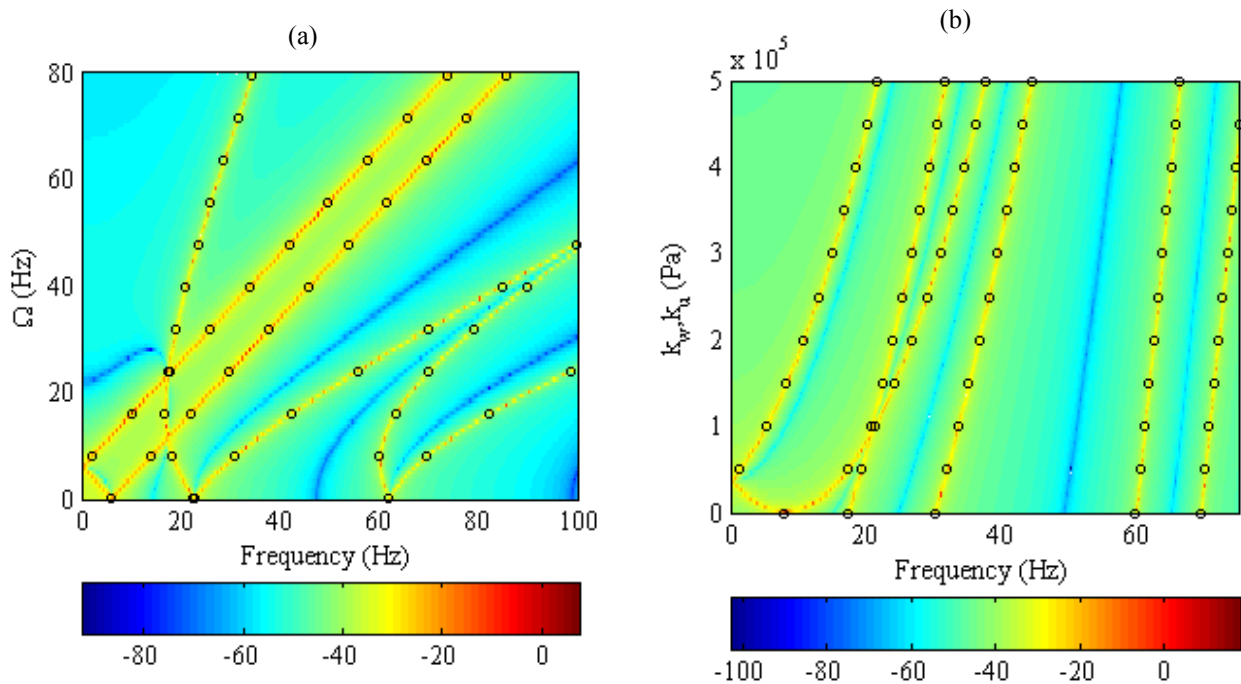


Figure 9. Map of FRF versus Ω with $k_w = k_q = 2 \cdot 10^4 \text{ N/m}^3$ (a) and map of FRF versus elastic foundation stiffness with $\Omega = 50 \text{ rad/s}$ (b): SEM (continuous map) and analytical solution (o).

5.3 Structural Damping

In this sub-section a structural damping of 0.01 with rotation speed of 50 rad/s is used. The internal pressure and elastic foundation effects are not considered.

The structural damping influences the real and imaginary parts of the wavenumbers that are zero or close to zero (Fig. 10a, Fig. 10b), increase them for larger values with increasing frequency, as a bifurcation respect to frequency. For higher damping values this characteristic is accentuated.

Figure 11 shows the structural damping decreases the amplitude of the resonance peaks without modifying the resonance frequencies. The amplitude of the rigid body mode contribution is not influenced and the amplitude of the peaks decreases with increasing frequency. At higher frequencies, because of the damping, only a resonance peak appears, leading to false impression that there is only one resonance instead of two.

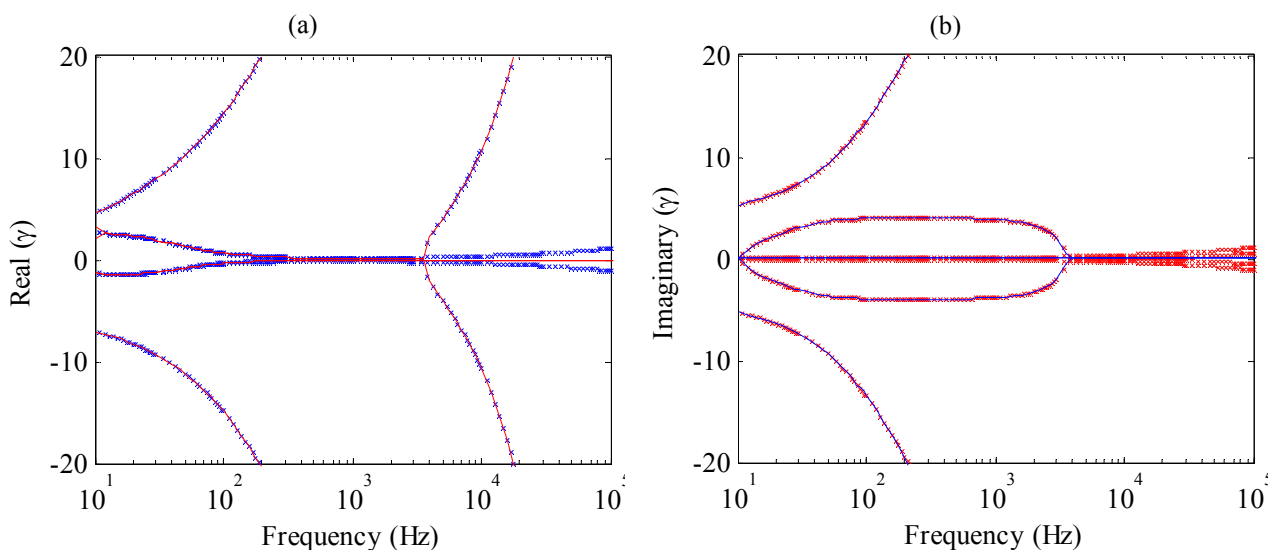


Figure 10. Real (a) and imaginary (b) parts of wavenumbers for $\eta = 0.01$ (x) and $\eta = 0$ (-).

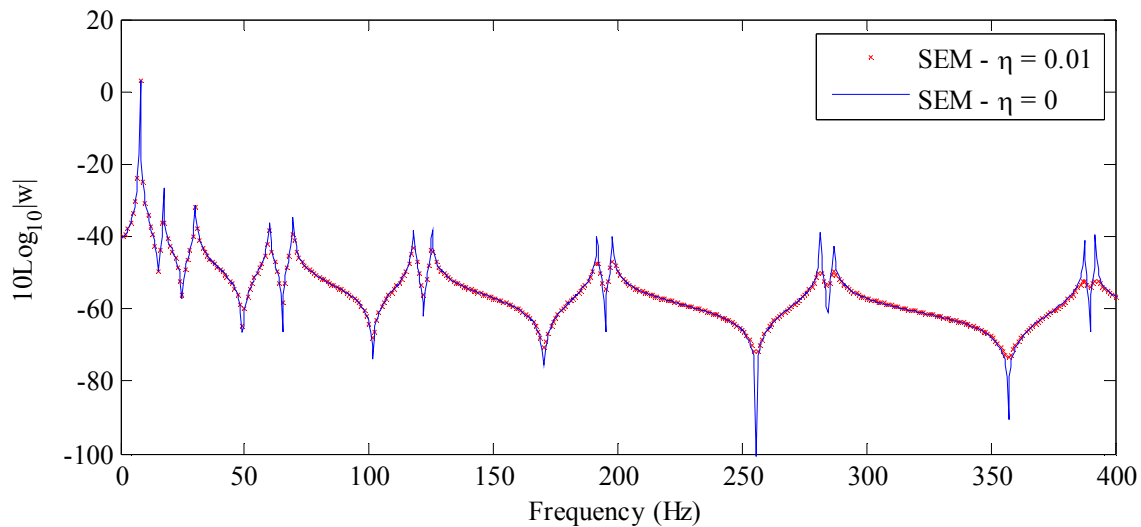


Figure 11. FRF for structural damping analysis: SEM for $\eta = 0.01$ (x) and SEM for $\eta = 0$ (-).

The map of FRF versus Ω with structural damping (Fig. 12a) has the same behavior of the map without structural damping. Only the amplitude of the resonances is smaller. In the map of FRF versus structural damping (Fig. 12b), it can be seen that the damping does not influence the resonances and that their amplitudes decrease with increasing damping

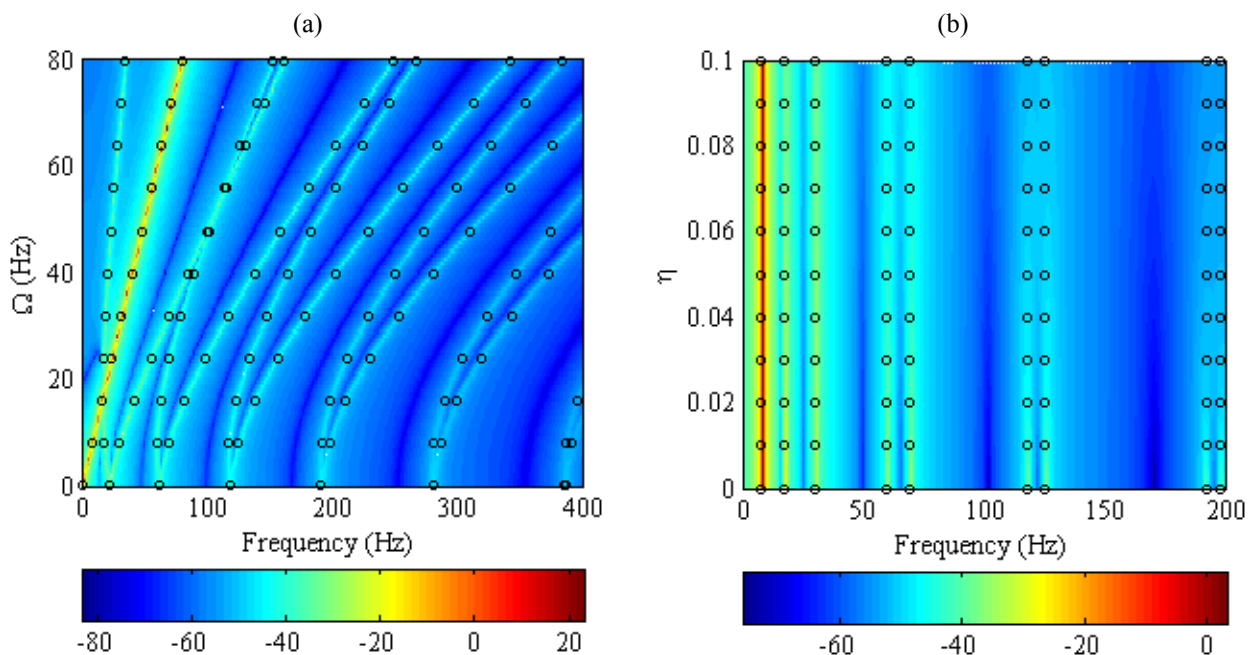


Figure 12. Map of FRF versus Ω with $\eta = 0.01$ (a) and map of FRF versus structural damping with $\Omega = 50$ rad/s (b): SEM (continuous map) and analytical solution (o).

6. CONCLUSIONS

This work developed a spectral element for a rotating ring with internal pressure, elastic foundation and structural damping. The spectrum relations, the forced responses and the maps in relation the parameters analyzed were obtained. The results were compared with the analytical solution and good agreement was obtained for all frequencies and in all the cases investigated.

The SEM model captures the physics of the dynamic problem including the rigid body mode effect, the bifurcations of the natural frequencies and the increase of the stiffness due the rotation. The internal pressure shifts the resonance peaks to higher frequencies making the system stiffer, the elastic foundation causes the bifurcation of the rigid body

D. Beli and J.R.F Arruda

Vibrations Analysis Of Rotating Ring With Internal Pressure And Elastic Foundation Using A Spectral Element Formulation

mode and also makes the system stiffer, and the structural damping decreases the amplitude of the resonance peaks without modifying the resonance frequencies.

The governing equations of motion for the analytical solution and SEM solution are the same, which explains the convergence of the results, but the analytical solution is only available to compute the free response of a uniform ring, while the SEM model can be used to compute the free and forced responses of a rotating ring with non-uniformities.

This study of SEM applied to rotating rings with internal pressure, elastic foundation and structural damping represents an improvement with respect to a previous investigation that considered only the rotation effects and is an original contribution to the literature on the subject. The physics of the dynamic phenomena involved could be represented and analyzed. Future work will introduce other effects in order to better describe the behavior of rings with non-uniformities.

7. ACKNOWLEDGEMENTS

The authors would like to thank CNPq (National Counsel of Technological and Scientific Development) for the financial support.

8. REFERENCES

- Beli, D. and Arruda, J.R.F, 2013. "Vibration Analysis of Rotating Ring Using a Spectral Element Formulation". In the *Proceedings of the XV International Symposium on Dynamic Problems of Mechanics – DINAME2013*. Buzios, Brazil.
- Bickford, W.B. and Reedy, E. S., 1985. "On the In-Plane Vibrations of Rotating Ring. *Journal of Sound and Vibration*". *Journal of Sound and Vibration*, Vol.101, p.13-22.
- Delamotte, J.C., Nascimento, R.F. and Arruda, J.R.F., 2008. "Simple models for the dynamic modeling of rotating tires". *Shock and Vibration*, Vol.15, p.383-393.
- Doyle, J. F., 1997. *Wave Propagation in Structure*. Springer, New York, 1st edition.
- Endo, M., Hatamura, K., Sakata, M. and Taniguchi, O., 1984." Flexural Vibrations of a Thin Rotating Ring". *Journal of Sound and Vibration*, Vol.92, p.261-272.
- Huang, S.C. and Soedel, W., 1987a. "Effects of Coriolis Acceleration on the Free and Forced In-Plane Vibrations of Rotating Rings on Elastic Foundation". *Journal of Sound and Vibration*, Vol.115, p.253-274.
- Huang, S.C. and Soedel, W., 1987b. "Response of Rotating Rings to Harmonic and Periodic Loading and Comparison with the Inverted Problem". *Journal of Sound and Vibration*, Vol.118, p.253-270.
- Lee, S.K., Mace, B.R. and Brennan, M.J., 2007. "Wave propagation, reflection and transmission in curved beams". *Journal of Sound and Vibration*, Vol.306, p.636-656.
- Lee, U., 2009. *Spectral Element Method in Structural Dynamic*. John Wiley & Sons, Singapore, 1st edition.

9. RESPONSIBILITY NOTICE

The authors are the only responsible for the printed material included in this paper.